PalmNet: Gabor-PCA Convolutional Networks for Touchless Palmprint Recognition

Angelo Genovese, *Member, IEEE,* Vincenzo Piuri, *Fellow, IEEE,*
Konstantinos N. Plataniotis, *Fellow, IEEE,* and Fabio Scotti, *Senior Member, IEEE*

***Abstract*—Touchless palmprint recognition systems enable high-accuracy recognition of individuals through less-constrained and highly usable procedures that do not require the contact of the palm with a surface. To perform this recognition, methods based on local texture descriptors and Convolutional Neural Networks (CNNs) are currently used to extract highly discriminative features while compensating for variations in scale, rotation, and illumination in biometric samples. In particular, the main advantage of CNN-based methods is their ability to adapt to biometric samples captured with heterogeneous devices. However, the current methods rely on either supervised training algorithms, which require class labels (e.g., the identities of the individuals) during the training phase, or filters pretrained on general-purpose databases, which may not be specifically suitable for palmprint data. To achieve a high recognition accuracy with touchless palmprint samples captured using different devices while neither requiring class labels for training nor using pretrained filters, we introduce PalmNet, which is a novel CNN that uses a newly developed method to tune palmprint-specific filters through an unsupervised procedure based on Gabor responses and Principal Component Analysis (PCA), not requiring class labels during training. PalmNet is a new method of applying Gabor filters in a CNN and is designed to extract highly discriminative palmprint-specific descriptors and to adapt to heterogeneous databases. We validated the innovative PalmNet on several palmprint databases captured using different touchless acquisition procedures and heterogeneous devices, and in all cases, a recognition accuracy greater than that of the current methods in the literature was obtained.**

***Index Terms*—Palmprint, Touchless Biometrics, Less-constrained, CNN, Deep Learning, PCA, Gabor.**

I. Introduction

BIOMETRIC systems recognize individuals based on their physiological or behavioral traits. Physiological traits include fingerprints, palmprints, and irises, whereas behavioral traits include a person's gait, voice, and signature [1]. In particular, palmprint-based biometric systems have been increasingly researched in recent years due to their high recognition accuracy, usability, and acceptability [2]–[4]. In fact, several palmprint acquisition systems rely on touchless, less-constrained, and highly usable acquisition procedures in which the position of the hand is not constrained and the palm does not touch any surface [5]–[10]. However, touchless palmprint images exhibit higher local differences in scale, rotation, translation, and illumination than touch-based images do, thereby increasing their intraclass variations and potentially reducing the recognition accuracy [2], [11].

To achieve accurate recognition using touchless images, several recent methods for biometric recognition have considered local texture descriptors that are designed to be robust to local changes in scale, rotation, translation, and illumination [12], [13]. The most recent approaches for palmprint recognition based on local texture descriptors generally involve computing a biometric template by extracting the local information related to the orientations of the lines on the palm [6], [14]–[16]. However, these approaches use handcrafted processing algorithms for feature extraction, using parameters whose optimal values may change for each database used based on the resolution and quality of the images [17]. Currently, there is no standard device for acquiring touchless palmprint samples, and the publicly available databases exhibit high differences in the resolution, quality, and dynamic range of the images [2].

Currently, numerous biometric approaches are being developed using techniques based on Deep Learning (DL) and Convolutional Neural Networks (CNNs) due to their ability to extract knowledge from noisy data, adapt to biometric samples captured using different devices, and achieve accurate recognition in less-constrained environments [17]–[20]. In particular, several approaches perform touchless and less-constrained palmprint recognition using CNNs [21]–[23]. However, the methods presented in the literature for palmprint recognition based on CNNs exhibit at least one or more of the following drawbacks. First, the majority of these methods use supervised training procedures, which require training data associated with corresponding class labels (e.g., the identities of the individuals associated with the palm images). Second, these methods use general-purpose filters that do not consider palmprint-specific features (e.g., filters pretrained on general image classification databases). Third, thorough experimental evaluations on multiple touchless palmprint databases are rarely performed, and hence, the ability of the CNNs to adapt to images captured with heterogeneous devices is not tested. Fourth, comparisons with recent methods based on local texture descriptors are generally not reported.

In this paper, to overcome the limitations of current CNNs

This work was supported in part by the Italian Ministry of Research as part of the MIUR PRIN project COSMOS (201548C5NT). We gratefully acknowledge the support of NVIDIA Corporation with the donation of the Titan X Pascal GPU used for this research, within the project "Deep Learning and CUDA for advanced and less-constrained biometric systems".

A. Genovese, V. Piuri, and F. Scotti are with the Department of Computer Science, Università degli Studi di Milano, 20133, Milan, Italy (e-mail: angelo.genovese@unimi.it, vincenzo.piuri@unimi.it, fabio.scotti@unimi.it).

K. N. Plataniotis is with the Department of Electrical and Computer Engineering, University of Toronto, M5S 3G4, Toronto, ON, Canada (e-mail: kostas@ece.utoronto.ca).

for palmprint recognition, we propose PalmNet[1], which is an innovative CNN that uses a novel method of applying Gabor filters in a CNN. PalmNet uses an innovative unsupervised training algorithm (i.e., an algorithm that does not require information about user identities) that can tune filters based on a limited quantity of data (e.g., ≈ 1000 images) using a new method based on Gabor responses and Principal Component Analysis (PCA). The proposed method has the following main advantages. First, the CNN does not require class labels during training; therefore, the model can be trained using privacy-preserving palmprint images that are not associated with the corresponding individuals. We use class labels only to evaluate the accuracy of the proposed method for biometric recognition and to compute the error metrics. Second, the CNN uses filters designed to be specific to palmprint data and adaptable to touchless palmprint databases captured with heterogeneous devices. A trained PalmNet has also the advantageous ability to extract a highly discriminative descriptor, which can be matched using various distance measures, from any palmprint sample. Because the model produces descriptors and not class labels, it is not necessary to train the CNN again when new individuals are added to the database.

The use of Gabor filters is motivated by their use in several recent works on palmprint recognition [2]. However, all previous palmprint recognition methods based on Gabor filters use a fixed set of filters with orientations obtained via constant sampling in the range $[0, \pi]$ and fixed values of scale, frequency, and standard deviation [24]. In this work, motivated by the fact that a finite set of Gabor filters with multiple scales and orientations can be used to represent any image [25], we propose a novel adaptive Gabor-based filter tuning procedure in which the scales and orientations of the filters are adapted to the considered samples to automatically obtain a CNN that can adapt to different databases and achieve a higher recognition accuracy than can be achieved with the current methods available in the literature. Although the use of Gabor filters in combination with CNNs has recently been proposed for general-purpose image classification [26], our approach is a novel method for the application of Gabor filters in a CNN that has the advantages of employing adaptive filters, extracting palmprint-specific features, and using an unsupervised CNN training procedure.

To test the validity of the method, we applied two variants of the proposed CNN to several public touchless palmprint databases captured with different acquisition procedures and devices, which contain images of different qualities, resolutions, and dynamic ranges. We also performed comparisons with several recent methods based on local texture descriptors and CNNs.

The main contributions of this work are as follows: *i)* it introduces PalmNet, a novel Gabor CNN for touchless palmprint recognition that achieves superior accuracy compared to other methods in the literature; *ii)* the proposed CNN is trained with an unsupervised procedure, which does not require class labels during training; *iii)* a new method of applying and tuning adaptive filters in a CNN is proposed, which is based on Gabor responses and PCA and is designed to be specific to palmprint data; *iv)* the first comprehensive comparison with major methods in the literature is performed by applying the proposed CNN to all major public touchless palmprint databases captured with heterogeneous devices and comparing its performance with the performance of recent methods in the literature based on texture descriptors and CNNs.

The remainder of this paper is structured as follows. Section II presents a detailed review of the related relevant techniques for touchless palmprint recognition. Section III introduces the proposed methodology based on PalmNet. Section IV describes the experimental results. Finally, Section V concludes the work.

II. Related Works

The current methods for touchless palmprint recognition can be divided into two-dimensional (2-D) and three-dimensional (3-D) methods based on the dimensionality of the processed samples. Although there are several methods that use 3-D palmprint models [5], [8], there are only a few publicly available databases for testing such methods. By contrast, there are many publicly available databases of 2-D palmprint images. Therefore, we focus on 2-D images in this work. It is possible to further divide 2-D palmprint recognition approaches into line-based, texture-based, subspace-based, coding-based, local-texture-descriptor-based, and DL-based approaches [7]. At present, approaches based on coding, local texture descriptors, and DL are most commonly studied in the literature and demonstrate the best recognition accuracies for palmprint recognition [2]. For this reason, we will focus on these three categories.

A. Coding-Based Approaches

Coding-based methods typically involve the application of a set of filters to an image, the quantization of the magnitudes or phases of the filter responses, and the encoding of the results to compute a biometric template. Then, global matching procedures based on the Hamming distance are used to compare the resulting templates [7]. Coding-based approaches can be divided into two classes: *i)* methods based on a single orientation and *ii)* methods based on multiple orientations. Table I presents a summary of coding-based methods for palmprint recognition.

The methods in class *i)* consider only the most relevant orientation for each region of the image. One such method is the PalmCode method described in [27], in which an image is processed using a single Gabor filter and the filter response is encoded for every pixel in the image. The Competitive Code method proposed in [30] improves upon PalmCode by considering multiple Gabor filters with different orientations and then encoding the index of the filter with the minimum response for each pixel, thus enabling the determination of the principal orientation of the palmprint lines at each point. Similarly, several other methods in the literature also use multiple filters and encode the most relevant responses, such as the Double-Orientation Code [32] and Robust Line Orientation Code [29] methods.

[1]The source code for PalmNet is available at http://iebil.di.unimi.it/palmnet/index.htm.

TABLE I
SUMMARY OF CODING-BASED APPROACHES FOR PALMPRINT RECOGNITION

Ref.	Year	Method	Class	Approach	Databases			Accuracy*
					Name	N. ind	N. samp.	
[27]	2003	PalmCode	*i)* Single orientation	Filters an image using a single Gabor filter and encodes the magnitude response for every pixel in the image.	PolyU [28]	386	7752	EER = 0.6%
[29]	2008	Robust Line Orientation Code	*i)* Single orientation	Filters an image using the Modified Finite Radon Transform (MFRAT) and encodes the most relevant response for each pixel. Performs matching based on pixel-to-area comparisons.	PolyU [28]	386	7752	EER = 0.4%
[30]	2010	Competitive Code	*i)* Single orientation	Filters an image using multiple Gabor filters with different orientations and encodes the index of the filter with the minimum response for each pixel. Performs matching based on angular distance.	PolyU [28] CASIA [31]	386 600	7752 5239	EER = 0.014% (PolyU) EER = 0.38% (CASIA)
[32]	2016	Double-Orientation Code	*i)* Single orientation	Filters an image using multiple Gabor filters with different orientations and encodes the indexes of the filters with the two most relevant responses for each pixel. Performs matching based on non-linear angular distance.	PolyU [28] IITD [33]	374 460	3740 2300	EER = 0.0092% (PolyU) EER = 0.0622% (IITD)
[34]	2009	Binary Orientation Co-occurrence Vector	*ii)* Multiple orientations	Filters an image using multiple Gabor filters with different orientations and encodes the responses of all Gabor filters for each pixel.	PolyU [28]	386	7752	EER = 0.0189%
[35]	2016	Neighboring Direction Indicator	*ii)* Multiple orientations	Filters an image using multiple Gabor filters with different orientations and, for each pixel, extracts the principal orientation and its relations to the orientations of the neighboring regions.	PolyU [28] IITD [33]	386 460	7752 2300	EER = 0.0225% (PolyU) EER = 0.0594% (IITD)
[36]	2018	Robust Competitive Code	*ii)* Multiple orientations	Filters an image using multiple Gabor filters with different orientations and, for each pixel, encodes the most relevant response along with the weighted responses for the neighboring orientations. Performs matching based on angular distance.	PolyU [28] IITD [33]	386 460	7752 2300	EER = 0.0189% (PolyU) EER = 0.0626% (IITD)

N. ind. = Number of individuals; N. samp. = Number of samples; EER = Equal Error Rate; * = As reported in the corresponding paper.

The methods in class *ii)* not only consider the principal orientation of the palmprint in each local zone but also extract a biometric template describing multiple orientations for each local region of the image. In the Binary Orientation Co-Occurrence Vector method described in [34], the responses of all Gabor filters are encoded for each pixel, while the Neighboring Direction Indicator (NDI) method proposed in [35] extracts the principal orientation for each pixel along with its relations to the orientations of the neighboring regions in the image. The Robust Competitive Code method described in [36] combines the Competitive Code approach with the NDI approach by encoding the most relevant response for each pixel along with the weighted responses for the neighboring orientations.

The main drawback of coding-based methods is that they involve comparing biometric templates using global matching methods based on the Hamming distance. Such global methods do not account for local variations in rotation and translation; therefore, they exhibit high recognition accuracies only on databases captured under partially constrained conditions, for example, using touch-based procedures. With the increasing popularity of touchless and less-constrained palmprint recognition systems [37], [38], several recent methods have been developed with a focus on local texture descriptors, which are more robust to local changes in rotation and illumination and therefore achieve higher recognition accuracies on touchless palmprint databases than coding-based methods do [2].

B. Local-Texture-Descriptor-Based Approaches

Methods based on local texture descriptors generally involve encoding the intensity value of each pixel, computing the histograms of the encoded representation (blockwise histograms) for each local region of the image, concatenating these blockwise histograms to obtain a one-dimensional feature vector representing the corresponding biometric template, and then using different distance measures (e.g., the Euclidean or chi-squared distance) to compare the resulting templates [47]. Local-texture-descriptor-based approaches can be divided into three classes: *i)* general-purpose descriptors applied to palmprint images, *ii)* texture descriptors encoding the main orientation for each pixel, and *iii)* texture descriptors encoding multiple orientations for each pixel. Table II presents a summary of local-texture-descriptor-based methods for palmprint recognition.

TABLE II
SUMMARY OF LOCAL-TEXTURE-DESCRIPTOR-BASED APPROACHES FOR PALMPRINT RECOGNITION

Ref.	Year	Method	Class	Approach	Databases			Accuracy*
					Name	N. ind	N. samp.	
[39]	2014	SIFT	*i)* General purpose	Combines the scale-invariant feature transform (SIFT) descriptor with random sample consensus (RANSAC) for outlier filtering.	IITD [33] CASIA [31]	470 624	2791 5502	EER = 0.4252% (IITD, left) EER = 0.4850% (IITD, right) EER = 0.3969% (CASIA, left) EER = 0.4897% (CASIA, right)
[40]	2006	LBP	*i)* General purpose	Uses the local binary patterns (LBP) descriptor for palmprint images. Performs matching based on an AdaBoost classifier.	UST [41]	574	5740	EER = 2%
[42]	2014	HOG	*i)* General purpose	Uses the histograms of oriented gradients (HOG) descriptor for palmprint images.	PolyU [28]	386	7752	R-1 rate = 98.03%
[43]	2016	LDP	*i)* General purpose	Uses the local directional patterns (LDP) descriptor for palmprint images. Performs matching based on chi-square distance.	PolyU [28] IITD [33] GPDS [44]	386 460 100	7752 2300 1000	EER = 0.0488% (PolyU) EER = 0.0751% (IITD) EER = 0.2929% (GPDS)
[15]	2017	LTrP	*i)* General purpose	Uses the local tetra patterns (LTrP) descriptor for palmprint images.	IITD [33] BERC	470 120	3290 8967	EER = 0.94% (IITD) EER = 1.49% (BERC)
[42]	2014	HOL	*ii)* Texture descriptors encoding the main orientation	Modifies the HOG texture descriptor to use either a bank of Gabor filters with different orientations or the MFRAT.	PolyU [28]	386	7752	R-1 rate = 99.95%
[6]	2017	CR-CompCode	*ii)* Texture descriptors encoding the main orientation	Combines Competitive Code with blockwise histograms. Performs matching based on a sparse representation classifier.	Tongji [45]	600	5182	R-1 rate = 98.78%
[16]	2016	LLDP	*iii)* Texture descriptors encoding multiple orientations	Uses either a bank of Gabor filters with different orientations or the MFRAT to compute the line responses for different orientations for each pixel, then encodes the maximum and minimum filtering responses for each pixel. Performs matching based on Manhattan and chi-square distances.	PolyU [28] Cross-Sensor [46] IITD [33]	386 200 459	7752 4000 2596	EER = 0.0216% (PolyU) EER = 1.470% (Cross-Sensor) EER = 4.07% (IITD)
[43]	2016	LMDP	*iii)* Texture descriptors encoding multiple orientations	Encodes multiple dominant directions for each pixel, considering the confidence of each dominant direction and the relations to the directions of neighboring regions.	PolyU [28] IITD [33] GPDS [44]	386 460 100	7752 2300 1000	EER = 0.0059% (PolyU) EER = 0.0264% (IITD) EER = 0.1847% (GPDS)
[15]	2017	LMTrP	*iii)* Texture descriptors encoding multiple orientations	Uses either a bank of Gabor filters or the MFRAT to determine the principal orientation for each pixel, then computes the horizontal and vertical derivatives at each pixel, considering a set of adjacent pixels for each derivative to account for the thickness of the palmprint lines.	IITD [33] BERC	470 120	3290 8967	EER = 0.87% (IITD) EER = 1.1119% (BERC)

Notes: N. ind. = Number of individuals; N. samp. = Number of samples; EER = Equal Error Rate; R-1 rate = Rank-1 identification rate, presented only when the paper does not report the EER; * = As reported in the corresponding paper.

In the methods of class *i)*, local texture descriptors designed for general-purpose applications are applied for palmprint recognition. Examples of general-purpose texture descriptors include the Scale-Invariant Feature Transform (SIFT) [7], [39], Local Binary Patterns (LBP) [40], Histograms of Oriented Gradients (HOG) [42], Local Directional Patterns (LDP) [43], and Local Tetra Patterns (LTrP) [15] descriptors. However, local texture descriptors designed specifically for palmprint recognition have recently been proposed that currently outperform general-purpose texture descriptors in most cases [16].

The methods of class *ii)* include the work described in [6], which introduces the Collaborative Representation Competitive Code (CR-CompCode) for palmprint recognition, a combination of a coding-based method and a local texture descriptor. In this method, the Competitive Code [30] approach is first applied, and blockwise histograms are then computed. Finally, a sparse representation classifier [48] is used for palmprint identification. However, this method has been tested only on high-quality images from a single palmprint dataset.

A modification of an existing approach is proposed in [42], which introduces the Histogram of Oriented Lines (HOL) descriptor, a modified version of the HOG texture descriptor [49] that uses either a bank of Gabor filters with different orientations or the Modified Finite Radon Transform (MFRAT). For each pixel, the magnitude and orientation of the minimum response are computed to extract the principal orientation; then, blockwise histograms are computed by dividing the magnitude responses into bins according to their orientations,

and these histograms are compared using the Euclidean distance. However, the drawback of the HOL descriptor is that it encodes only the principal orientation for each pixel, whereas more recent methods typically consider multiple orientations.

The Local Line Directional Patterns (LLDP) descriptor proposed in [16] considers multiple orientations and belongs to class *iii)*. This method is based on the LDP texture descriptor [50] and uses either a bank of Gabor filters with different orientations or the MFRAT to compute the line responses for different orientations for each pixel. Then, the maximum and minimum filtering responses are encoded for each pixel, corresponding blockwise histograms are computed, and various distance measures are used to compare the resulting templates. Similarly, [43] introduces the Local Multiple Directional Patterns (LMDP) descriptor, which is an extension of the LLDP descriptor that, for each pixel, considers multiple dominant directions, the confidence of each dominant direction, and the relations to the directions of neighboring regions.

In addition to considering multiple orientations for each pixel, the method described in [15] considers the different thicknesses of the palmprint lines. In this method, the LTrP texture descriptor [51] is extended to the Local Microstructure Tetra Patterns (LMTrP) descriptor, which uses either a bank of Gabor filters or the MFRAT to determine the principal orientation for each pixel. Then, the horizontal and vertical derivatives are computed at each pixel; for each derivative, a set of adjacent pixels is considered to account for the thickness of the palmprint lines. In this approach, the results of the two derivatives are encoded into a 2-bit number for each pixel; these numbers are then processed using the LBP descriptor, corresponding blockwise histograms are computed, and the resulting histograms are compared using the Euclidean distance.

The LLDP, LMDP, and LMTrP descriptors are currently the most accurate local texture descriptors for touchless palmprint recognition. However, their calculation requires handcrafted feature extraction procedures that involve manually tuning a large number of parameters. To overcome the drawbacks of local texture descriptors, several palmprint recognition systems have recently been proposed based on the use of DL and CNN techniques due to their ability to natively process input images and adapt to samples captured with heterogeneous devices.

C. Deep-Learning-Based Approaches

In DL-based approaches for palmprint recognition, a CNN is generally used to extract features from the images, and a distance measure or a trained classifier is then used to compare the resulting biometric templates. DL-based approaches can be divided into three classes: *i)* methods using pretrained CNNs, *ii)* methods using CNNs trained on palmprint images, and *iii)* methods using CNNs with fixed filters. Table III presents a summary of DL-based methods for palmprint recognition.

One of the methods of class *i)* is the work presented in [52], which is based on a comparison among several pretrained CNNs. Feature extraction from touchless palmprint images is performed using pretrained AlexNet, VGG-16, and VGG-19 networks; subsequently, classification is performed using a support vector machine (SVM). The results show that the deeper networks, VGG-16 and VGG-19, obtain better results than those of AlexNet. However, classification is performed using an SVM trained with a supervised procedure, and no comparisons with other methods in the literature are presented. Similarly, the method described in [21] combines a pretrained AlexNet with an SVM to identify the palmprints of newborns captured using a touchless procedure. Although the method performs better than coding-based methods do, it also relies on an SVM trained with a supervised procedure, and no comparisons with techniques based on texture descriptors are presented.

The approach described in [23] belongs to class *ii)* and uses a CNN based on the AlexNet model [58] and trained on palmprint images by optimizing a loss function describing the separation of the genuine and impostor distributions. The method demonstrates superior performance compared with recent coding-based methods; however, it relies on a supervised training procedure, and no comparisons with local-texture-descriptor-based methods are presented, although testing was performed on touchless palmprint databases.

A method based on PCANet [59], a CNN trained using an unsupervised PCA-based procedure, is proposed in [22]. In this approach, PCANet is applied to extract features from palmprint images, and a trained classifier (e.g., an SVM) is then used for classification. The method achieves results similar to those of most recent methods in the literature; however, although it is suitable for use with various classifiers, all of them are trained using supervised procedures, and only applications based on multispectral databases have been proposed.

The methods of class *iii)* include the deep scattering network presented in [56], which processes input images using a bank of fixed filters based on the scattering transform [60]; then, an SVM is used to classify the palmprint images. However, this method also uses a supervised training procedure, and again, no comparisons with recent works based on local texture descriptors are presented.

The main drawbacks of DL-based methods for palmprint recognition are as follows. The CNNs are often combined with classifiers trained using supervised training procedures (e.g., SVMs) for classification. The models used have often been trained for general-purpose applications (e.g., AlexNet or a deep scattering network), or the training procedures are not designed to extract palmprint-specific features (e.g., PCANet). Moreover, extensive comparisons with recent methods in the literature, either coding-based or local-texture-descriptor-based methods, are rarely performed.

III. Methodology

In the proposed approach, touchless palmprint images are recognized by using PalmNet, which is a novel Gabor CNN based on both fixed and adaptive filters. The CNN is trained using a novel unsupervised procedure for filter tuning based on Gabor responses and PCA, without requiring class labels (e.g., the identities of the users). We use class labels only to evaluate the accuracy of the proposed method for biometric recognition and to compute the error metrics. The network is capable of adapting to different databases captured using heterogeneous

TABLE III
SUMMARY OF DL-BASED APPROACHES FOR PALMPRINT RECOGNITION

Ref.	Year	Method	Class	Approach	Databases			Accuracy*
					Name	N. ind	N. samp.	
[52]	2018	AlexNet, VGG-16, VGG-19	*i)* Pretrained CNNs	Performs feature extraction using pre-trained CNNs. Performs classification based on a support vector machine (SVM).	MOHI [53] COEP [54]	200 168	3000 1344	R-1 rate $\approx 95.5\%$ (MOHI, COEP)
[21]	2018	AlexNet	*i)* Pretrained CNNs	Performs feature extraction using a pre-trained CNN and then classifies samples using an SVM.	CPNB [21]	100	2000	EER $= 3.03\%$
[23]	2016	AlexNet, Discriminative Index Learning	*ii)* CNNs trained on palmprint images	Uses a CNN based on the AlexNet model and trained by optimizing a loss function describing the separation of the genuine and impostor distributions.	IITD [33] CASIA [31]	460 624	2300 5502	EER $= 1.64\%$ (IITD) EER $= 1.86\%$ (CASIA)
[22]	2017	PCANet	*ii)* CNNs trained on palmprint images	Uses a CNN with filters learned from input images via an unsupervised PCA-based procedure.	CASIA$_{wht}$ [55]	200	1200	EER $= 0.299\%$
[56]	2017	Deep Scattering Network	*iii)* CNNs with fixed filters	Uses a newly proposed deep scattering network based on the scattering transform to process input images using fixed filters. Performs classification based on an SVM.	PolyU [57]	500	6000	R-1 rate $= 99.9\%$

Notes: N. ind. = Number of individuals; N. samp. = Number of samples; EER = Equal error rate; R-1 rate = Rank-1 identification rate, considered only when the paper does not report the EER; * = As reported in the corresponding paper.

devices and extracting highly accurate palmprint-specific features, thereby achieving a greater recognition accuracy than can be achieved using the methods available in the literature. PalmNet can be applied to any segmented palmprint image and outputs a biometric template consisting of a 1-D feature vector. It is then possible to use any classifier or distance measure to compare the resulting biometric templates. In this work, to demonstrate the validity of PalmNet for extracting highly discriminative features, we classify the generated templates using a k-Nearest-Neighbors (k-NN) classifier with $k = 1$ based on the Euclidean distance, which has no parameters and does not require a training procedure [61].

The method consists of the following steps: *A)* preprocessing, *B)* CNN training, *C)* feature extraction, and *D)* classification and matching. Fig. 1 presents the outline of the proposed method.

A. Preprocessing

In the preprocessing step, the Region Of Interest (ROI) is extracted from a grayscale palmprint image. This step can be divided into three individual tasks: *i)* hand segmentation, *ii)* valley point extraction, and *iii)* ROI computation. Fig. 2 presents an example of an ROI extracted from a touchless palmprint image.

First, we convert the input color image to grayscale, remove the background, and extract the contour of the hand using a procedure based on Otsu thresholding and the Kirsch edge detector [62]. Several works in the literature on palmprint recognition have proposed skin-color-based segmentation methods for samples captured with an unconstrained background using touchless acquisition systems [63]–[65] or mobile devices [66], [67]. However, in this work, we consider grayscale palmprint samples captured with a uniform background; therefore, it is not necessary to use color-based techniques to segment the samples. Instead, we focus on hand segmentation methods based on gray-level thresholding and edge detection.

Second, from the hand contour, we extract the valley points corresponding to the intersections between the index, middle, ring, and little fingers by analyzing the local minima of the contour following a combination of the procedures described in [64], [68], [69].

Third, we compute the ROI by establishing a reference system based on the extracted valley points using the procedure proposed in [5]. We resize the ROI to dimensions of $u \times v$ pixels and normalize it by subtracting the mean value.

B. CNN Training

In this section, we describe the procedure for the unsupervised training of the proposed PalmNet. First, we introduce the network topology, and then we describe the procedures used to tune the filters based on Gabor responses and PCA. Finally, we define the parameters of the proposed CNN.

1) Network Topology: The proposed PalmNet is a 3-layer CNN with 2 convolutional layers (L_1 and L_2) and 1 binarization layer (L_3). Fig. 3 shows the topology of the CNN. The layers are configured as follows:

- L_0: Input layer with dimensions of $u \times v$, corresponding to the size of the palmprint ROI.
- L_1: First convolutional layer, composed of k_1 filters. Each filter is used to process the input image; thus, the output of this layer consists of k_1 images with dimensions of $u \times v$.
- L_2: Second convolutional layer, composed of k_2 filters. Each filter is used to process each of the k_1 images output by layer L_1. Thus, the output of this layer consists of $k_1 k_2$ images with dimensions of $u \times v$.

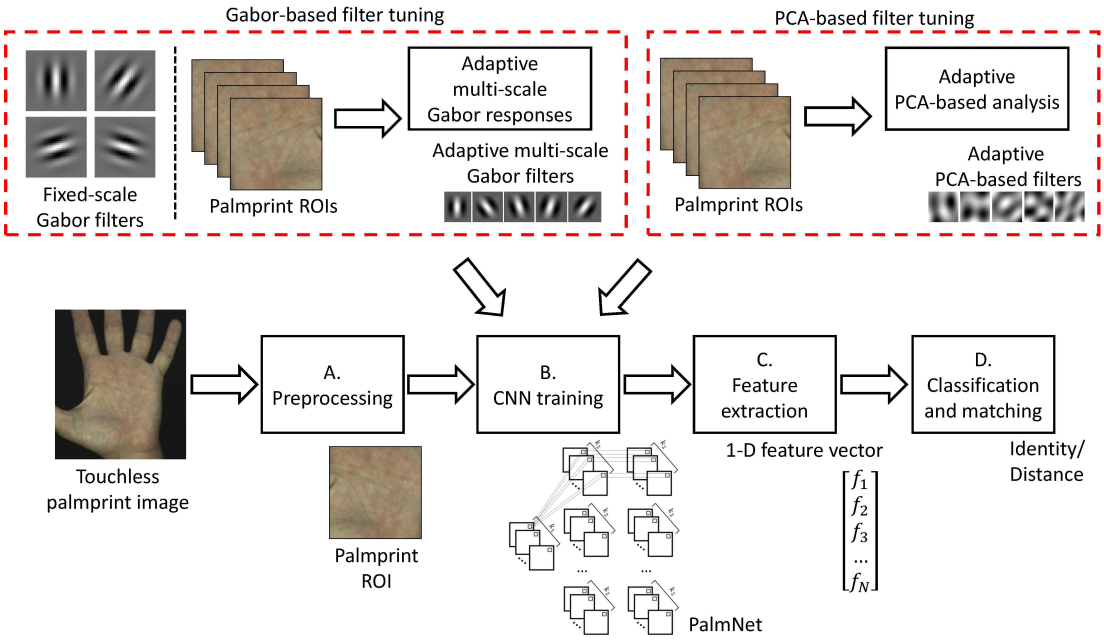

Fig. 1. Outline of the proposed palmprint recognition method based on PalmNet, a CNN trained using an unsupervised procedure to tune the filters based on Gabor responses and PCA.

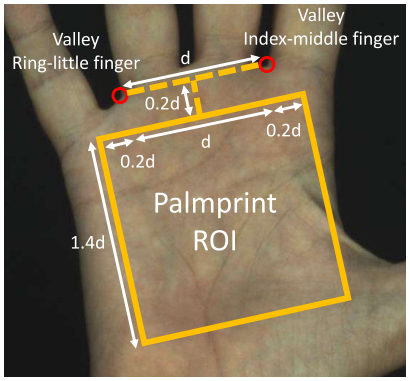

Fig. 2. Example of a reference system based on extracted valley points and the corresponding computed ROI.

- L_3: Binarization layer that applies the function $f(x) = \text{bin}(x)$ to every pixel of the $k_1 k_2$ images output by layer L_2, where $\text{bin}(x)$ is defined by the following equation:

$$\text{bin}(x) = \begin{cases} 1 & \text{if } x > 0 \\ 0 & \text{otherwise} \end{cases} . \quad (1)$$

  The output of this layer consists of $k_1 k_2$ binary images with dimensions of $u \times v$. The purpose of the binarization layer is to allow the size of the L_2 output to be reduced by combining several outputs into single decimal numbers [16], [59]. By using the binarization layer output, k_2 outputs can be thresholded to binary digits and combined into a single decimal number, as described in Section III-C.

The filters in layers L_1 and L_2 have variable sizes and are configured using unsupervised training procedures. In the proposed method, we consider two kinds of adaptive filters. First, we consider Gabor filters, which are currently used in several state-of-the art palmprint recognition methods due to their ability to enhance palmprint lines, thus ensuring that only significant biometric details are extracted [6], [15], [16]. Second, we consider PCA-based filters, which have been successfully used in several fields, including biometric recognition based on faces and palmprints [22], [59], [70], [71]. The main difference between the PCA-based and Gabor filters is that the PCA-based filters do not rely on any shape assumption and are trained entirely via the proposed PCA-based tuning procedure, whereas the Gabor filters are specific to palmprint characteristics and assume a shape defined by the product of a sinusoidal wave with a Gaussian function [15], [16].

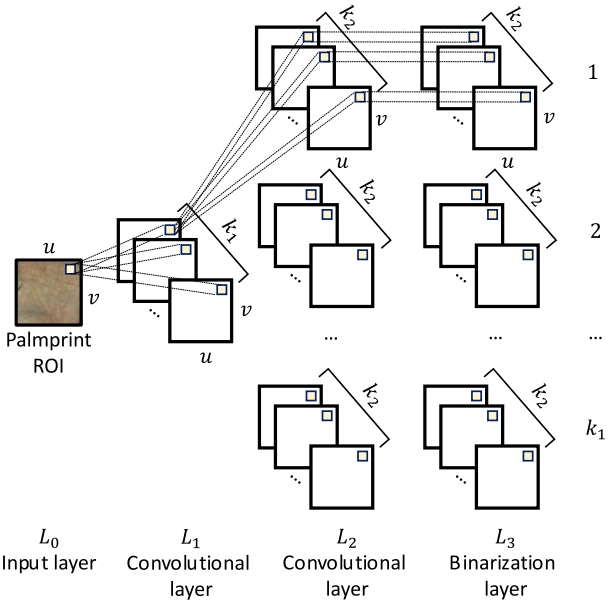

Fig. 3. Topology of the proposed PalmNet.

In this work, we propose two Gabor CNNs, PalmNet-Gabor and PalmNet-GaborPCA, in order to separately evaluate the contributions of the Gabor and PCA-based filter tuning procedures. The two Gabor CNNs are structured as follows.

- *PalmNet-Gabor*: The k_1 filters of layer L_1 and the k_2 filters of layer L_2 are configured using the Gabor-based tuning procedure described in Section III-B2.
- *PalmNet-GaborPCA*: The k_1 filters of layer L_1 are configured using the PCA-based tuning procedure described in Section III-B3, and the k_2 filters of layer L_2 are configured using the Gabor-based tuning procedure described in Section III-B2.

2) Gabor-Based Filter Tuning: Fig. 4 shows the outline of the proposed Gabor-based filter tuning procedure. Specifically, the tuning procedure configures two types of filters: *i)* fixed-scale Gabor filters and *ii)* adaptive multiscale Gabor filters.

a) Fixed-Scale Gabor Filters: We create a set of fixed-scale 2-D Gabor filters, denoted by G_f, as products of a sinusoidal wave with a Gaussian function, based on the filters used in recent local texture descriptors for palmprint recognition [15], [16]. These filters have the following fixed-scale form:

$$G_f(x, y, \theta, \mu, \sigma) = \frac{1}{2\pi\sigma^2} \exp\left(-\frac{x^2+y^2}{2\sigma^2}\right) \exp(2\pi j(\mu x \cos\theta_f + \mu y \sin\theta_f)) \ , \quad (2)$$

where $j = \sqrt{-1}$, μ represents the frequency of the sinusoidal wave, σ is the standard deviation of the Gaussian function, and θ_f is the orientation of the filter. We use fixed values for μ and σ, and for the orientation θ_f, we use values sampled from the set Θ_f, which is computed using the following equation:

$$\Theta_f = \left\{ \theta_f \middle| \theta_f = i\frac{\pi}{F} \right\}, \quad i = 1, \dots F \ . \quad (3)$$

Thus, we obtain a set G_f of F fixed-scale 2-D Gabor filters with dimensions of $h_1 \times h_2$. Fig. 5a shows the bank of fixed-scale Gabor filters computed using the proposed approach.

b) Adaptive Multiscale Gabor Filters: To compute the set of adaptive multiscale Gabor filters, we use a training subset of palmprint ROIs. First, we compute a set of adaptive orientations from the palmprint ROIs. Second, we compute a bank of multiscale Gabor filters with the computed orientations. Third, we select the filters that obtain the greatest magnitude responses.

- *Computation of adaptive orientations:* We perform low-pass filtering on each ROI and apply a gradient-based operator to determine the image I_{Orient} that describes the local directions of the texture pattern. Then, we compute the histogram of I_{Orient}, take the average of the histograms thus computed for all training ROIs, and extract the S most frequent orientations Θ_s. A set of C adaptive orientations, Θ_c, is obtained as $\Theta_c = \Theta_s \cup \Theta_f$, where Θ_f is computed using Eq. 3 and $C = |\Theta_c|$, with $|\cdot|$ denoting the cardinality of the set.
- *Computation of multiscale Gabor filters*: We define two sets of even-symmetric and odd-symmetric multiscale 2-D Gabor filters, $G_{a,even}$ and $G_{a,odd}$, respectively, using the following equations [25]:

$$\begin{aligned} &G_{a,even}(x_{rot}, y_{rot}, \theta_c, m_f) = \\ &\text{real}\left(a_0^{-m_f}\frac{1}{\sqrt{2}}\exp\left(\frac{-1}{2r^2}\left(r^2 x_{rot}(\theta_c)^2 + y_{rot}(\theta_c)^2\right)\right)\right. \\ &\left.\left(\exp\left(jkx_{rot}(\theta_c)\right) - \exp\frac{-k^2}{2}\right)\right) \ ; \\ &G_{a,odd}(x_{rot}, y_{rot}, \theta_c, m_f) = \\ &\text{imag}\left(a_0^{-m_f}\frac{1}{\sqrt{2}}\exp\left(\frac{-1}{2r^2}\left(r^2 x_{rot}(\theta_c)^2 + y_{rot}(\theta_c)^2\right)\right)\right. \\ &\left.\exp\left(j\psi x_{rot}(\theta_c)\right)\right) \ , \end{aligned} \quad (4)$$

where $\text{real}(\cdot)$ and $\text{imag}(\cdot)$ denote the real and imaginary parts of the argument, which are used to obtain the even- and odd-symmetric filters, respectively; a_0 is a scaling factor; r defines the aspect ratio of the filter; and ψ represents the frequency. The value m_f controls the scale of the filter and is computed as follows:

$$m_f = [0, 1, \dots, ...M] \ , M = \lceil log_2(u/2) \rceil \ , \quad (5)$$

where u is the horizontal size of the ROI. Then, we define $x_{rot}(\theta_c)$ and $y_{rot}(\theta_c)$ using the following equations:

$$\begin{aligned} x_{rot}(\theta_c) &= \left(a_0^{-m_f}x - \frac{(4+2^{-m_f})}{2}\right)\cos\theta_c + \\ &\quad \left(a_0^{-m_f}y - \frac{(4+2^{-m_f})}{2}\right)\sin\theta_c \ ; \\ y_{rot}(\theta_c) &= -\left(a_0^{-m_f}x - \frac{(4+2^{-m_f})}{2}\right)\sin\theta_c + \\ &\quad \left(a_0^{-m_f}y - \frac{(4+2^{-m_f})}{2}\right)\cos\theta_c \ , \end{aligned} \quad (6)$$

with $\theta_c \in \Theta_c$. In total, we obtain a set $G_{a,even}$ containing $A = M \cdot C$ even-symmetric multiscale filters and another set $G_{a,odd}$ containing $A = M \cdot C$ odd-symmetric multiscale filters. The filter size is computed as $g_1 \times g_2 = 4 \cdot 2^{m_f}$. Fig. 5b,c show the bank of multiscale Gabor filters computed using the proposed approach.

- *Selection of the filters with the greatest magnitude responses*: We adapt the multiscale Gabor filters to the training data by selecting the most relevant filters based on their magnitude responses. First, we filter the ROI image I with each filter in the sets $G_{a,even}$ and $G_{a,odd}$, thus obtaining two sets of filtered images $\{I_{a,even}\}$ and $\{I_{a,odd}\}$, and for each corresponding pair of filtered images, we compute the combined magnitude response as $I' = I^2_{even} + I^2_{odd}$, thus obtaining a set of images $\{I'_a\}$. Second, we sort the magnitude responses for all pixels in $\{I'_a\}$ to obtain a 1-D vector $\mathbf{s_m}$ of size $A \cdot u \cdot v$, which contains the magnitude responses in decreasing order. Then, for each filter in G_a, we count the number of corresponding responses in $\mathbf{s_m}$, considering each filter at most once for each position (x, y) in the ROI. Third, we count the number of occurrences for each filter among all ROIs, and we extract the A' filters $G_{a',even}$ and $G_{a',odd}$

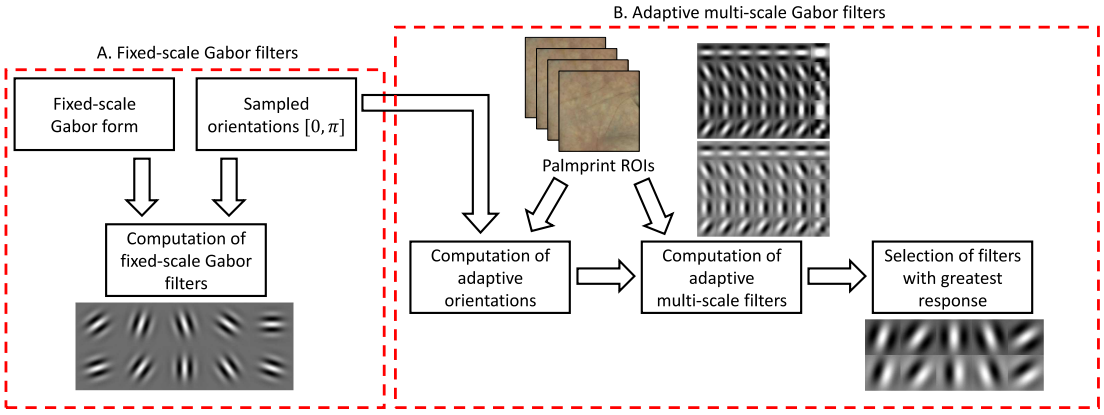

Fig. 4. Outline of the proposed Gabor-based filter training procedure. Two types of filters can be distinguished: *A)* fixed-scale Gabor filters and *B)* adaptive multiscale Gabor filters.

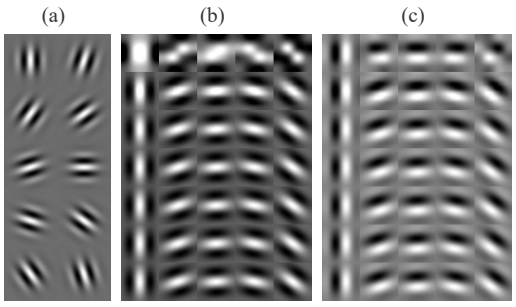

Fig. 5. Complete set of Gabor filters used in the proposed PalmNet: (a) fixed-scale Gabor filters, (b) even-symmetric multiscale Gabor filters, and (c) odd-symmetric multiscale Gabor filters. Each row of images in (b,c) contains filters computed with the same scale m_f. For each scale, we sampled 5 orientations for visualization purposes. The Gabor-based filter tuning procedure then adapts the multiscale Gabor filters to the training data by selecting the most representative A' filters for each database.

with the most occurrences from $G_{a,even}$ and $G_{a,odd}$, respectively.

The output of the Gabor-based filter tuning procedure consists of $F + A'$ filters, corresponding to F fixed-scale 2-D Gabor filters and A' adaptive multiscale 2-D Gabor filters. The numbers of fixed and adaptive Gabor filters can be chosen based on the CNN topology and the number of filters chosen for each layer of the network, i.e., k_1 and k_2.

3) PCA-Based Filter Tuning: The unsupervised PCA-based filter tuning procedure consists of the following two steps [59]: *i)* collection of local regions of the ROIs to construct the unsupervised dataset and *ii)* PCA computation and extraction of the filters of the CNN as the PCA eigenvectors.

First, we extract local regions $p_{i,j}$ with dimensions of $m_1 \times m_2$ centered on each pixel of the ROI, with $i = 1, 2, \ldots, u$ and $j = 1, 2, \ldots, v$, where u and v are the vertical and horizontal sizes, respectively, of the ROI. A local region is extracted for each pixel, thus covering every part of the ROI. We transform these local regions into vector form, thus obtaining $u \cdot v$ vectors $\mathbf{p_1}, \mathbf{p_2}, \ldots, \mathbf{p_{uv}} \in R^{m_1 m_2}$, and from each vector, we subtract its mean value. Then, we compute a matrix $P \in R^{m_1 m_2 \times Nuv}$ by concatenating the vectors $\mathbf{p_i}$ for each of the N ROIs.

Second, we perform the PCA computation for P by computing PP^T and extracting the V principal eigenvectors of PP^T, denoted by $\mathbf{e_i}$, with $i = 1, 2, \ldots, V$. We extract the V corresponding filters of the CNN by transforming each eigenvector $\mathbf{e_i}$ into a matrix $E_i \in R^{m_1 \times m_2}$. The number of filters V can be chosen based on the CNN topology and the number of filters chosen for each layer of the network, i.e., k_1 and k_2.

TABLE IV
SUMMARY OF THE PARAMETERS OF THE PROPOSED CNNS

Network	Parameter(s)	Value(s)	Description
PalmNet-Gabor	u, v	128, 128	Horizontal and vertical sizes of the palmprint ROI
	h_1, h_2	35, 35	Dimensions of the fixed-scale Gabor filters
	μ	0.11	Wavelength of the fixed Gabor filters
	σ	5.6179	Standard deviation of the fixed Gabor filters
	k_1	15	Number of filters in L_1
	k_2	15	Number of filters in L_2
	F	10	Number of fixed-scale Gabor filters
	A'	5	Number of adaptive multiscale Gabor filters
	S	10	Number of most frequent orientations
	a_0	2	Scaling factor of the adaptive multiscale Gabor filters
	r	1	Aspect ratio of the adaptive multiscale Gabor filters
	ψ	2.4653	Frequency of the adaptive multiscale Gabor filters
PalmNet-GaborPCA	m_1, m_2	15, 15	Dimensions of the PCA-based filters
	k_1	15	Number of filters in L_1
	k_2	15	Number of filters in L_2
	V	15	Number of principal eigenvectors from PCA

4) Network Parameters: We experimentally tuned some of the network parameters to achieve the best possible recognition accuracy on the considered datasets while respecting the memory requirements of the proposed algorithms, and we selected the other parameters by considering the optimal values found in the literature, following the procedure described in Section IV-C. We summarize the parameters of the CNNs used in this work in Table IV.

C. Feature Extraction

The feature extraction step can be divided into the following three individual tasks: *i)* applying the trained CNN, *ii)* encoding the binary images, and *iii)* computing the feature vector based on the histogram.

First, we apply the trained CNN (either PalmNet-Gabor or PalmNet-GaborPCA, depending on the chosen topology) to a palmprint ROI. Thus, we obtain $k_1 k_2$ binary images, as described in Section III-B1. Specifically, each group of k_2 binary images in the output of layer L_3 corresponds to one of the k_1 images in the output of layer L_1, as shown in Fig. 3. Thus, there are k_1 groups in total, each containing k_2 images.

Second, we consider one group of k_2 binary images, denoted by B_i, with $i = 1, 2, \ldots, k_2$. Each of the k_2 images in the group has the same dimensions of $u \times v$. For each position (x, y), we construct a binary vector $\mathbf{b}$ by concatenating the binary values of all k_2 images using the following equation: $\mathbf{b} = [B_1(x, y), B_2(x, y), \ldots, B_{k_2}(x, y)]$. We then encode the binary vector $\mathbf{b}$ into a decimal number d as follows: $d = \sum_{j=1}^{k_2} 2^{j-1}\mathbf{b}(j)$. We repeat this encoding process for each position (x, y) to obtain a decimal matrix $D(x, y)$ that describes the entire group of k_2 binary output images. In the same way, we compute the decimal matrices D_l for all k_1 groups of binary images, with $l = 1, 2, \ldots, k_1$.

Third, we divide each image D_l into n_B nonoverlapping blocks with dimensions of $b_1 \times b_2$ and compute a corresponding histogram for each block, where each histogram consists of 2^{k_2} bins. Finally, we construct a feature vector H by concatenating the histograms for all blocks of all images D_l, where $|H| = 2^{k_2} k_1 n_B$. We experimentally tuned the values of b_1 and b_2 to achieve the best possible recognition accuracy on the considered datasets following the procedure described in Section IV-C.

D. Classification and matching

The proposed method can be applied in both identification and verification modes [1]. In the identification mode, a classification step is performed, in which the set of feature vectors $\{H\}$ extracted from the palmprint ROIs is taken as the input to compute the class (identity) associated with each feature vector. In the literature, several types of classifiers have been considered, including classifiers based on SVMs, neural networks, pretrained CNNs, and sparse representations [20]. In this work, to evaluate the ability of PalmNet to extract highly discriminative feature vectors, we use a simple k-NN classifier based on the Euclidean distance, with $k = 1$ (denoted by 1-NN in the following), which does not need to be trained and has no parameters to tune [61].

In the verification mode, a matching step is performed, in which two biometric templates represented by feature vectors H_1 and H_2 are compared to compute a corresponding distance $d_{1,2} = match(H_1, H_2)$, where $match(\cdot)$ is the Euclidean distance.

IV. Experimental Results

This section presents the touchless palmprint databases considered in our study, introduces the evaluation procedure and the error metrics used to compare the recognition accuracy, describes the procedure used to tune the network parameters, provides a visual examination of the filter tuning procedure, and then reviews the recognition accuracy of the proposed CNNs. Specifically, we performed a technology evaluation [72] to compare the recognition accuracy of the proposed method with the accuracies of the most recent methods in the literature. Finally, this section presents the computation time and feature size of the proposed approach.

TABLE V
Summary of the databases used in this study

Ref.	Name	Methodology	N. ind.	N. samp.
[31]	CASIA	Users place their hands inside a box with controlled illumination and place the back of the hand on a fixed surface.	624	5455
[33]	IITD	Users place their hands inside a box with controlled illumination and place the back of the hand on a fixed surface.	467	2669
[73]	REST	Users place the back of the hand on a fixed surface with no enclosure; the only illumination is provided by environmental indoor lighting.	358	1937
[6]	Tongji	Users place their hands inside an enclosure; the hand does not touch any surface, the illumination is controlled, and the position of the hand can vary within a small space.	600	5182

Notes: N. ind. = Number of individuals; N. samp. = Number of samples.

A. Databases Used

To evaluate the recognition accuracy of the proposed method, we considered 4 touchless palmprint databases captured under different conditions with heterogeneous devices. All of the databases are publicly available. For every database, we considered the left and right palms of the same person as belonging to different individuals. We computed the ROIs by applying the preprocessing step described in Section III-A and discarded only a small fraction of images for which the preprocessing algorithm could not extract the valley points. Table V presents an overview of the databases used in this study.

1) CASIA Palmprint Database V1: The CASIA Palmprint Database V1 (referred to as CASIA in the remainder of this section), collected by the Institute of Automation of the Chinese Academy of Sciences, contains 5486 palmprint samples captured from 624 individuals, both male and female. The images were captured using the proprietary touchless acquisition device described in [31]. They are in 8-bit grayscale and have dimensions of 640×480. Each user was required to place his or her hand inside a box with controlled illumination and place the back of the hand on a fixed surface. Consequently, the hand is oriented in approximately the same direction in all samples. After the preprocessing step, only $\approx 0.5\%$ of the samples were discarded. A total of 5455 ROIs were considered in our experiments.

2) IIT Delhi Touchless Palmprint Database (Version 1.0): The IIT Delhi Touchless Palmprint Database (Version 1.0) (referred to as IITD), collected by the Indian Institute of Technology Delhi, contains 2769 palmprint samples captured

from 467 individuals recruited from among the students and staff of IITD, with ages ranging from 12 to 57 years. The images were captured using the proprietary touchless acquisition device described in [33]. They are in 8-bit grayscale and have dimensions of 800×600. Each user was required to place his or her hand inside a box with controlled illumination and place the back of the hand on a fixed surface. Consequently, the hand is oriented in approximately the same direction in all samples. After the preprocessing step, only $\approx 3.5\%$ of the samples were discarded. A total of 2669 ROIs were considered in our experiments.

3) REgim Sfax Tunisia (REST) hand database 2016: The REgim Sfax Tunisia (REST) hand database 2016 (referred to as REST), collected by the Research Groups in Intelligent Machines of Sfax University, contains 1945 palmprint samples captured from 358 individuals with ages ranging from 6 to 70 years. The images were captured using a low-cost digital camera following the procedure described in [73]. They are in 24-bit color and have dimensions of 2048×1536. The position of the hand is less constrained than in the CASIA and IITD databases since no enclosure was provided in which the users were required to place their hands, and illumination was provided only by environmental indoor lighting. Consequently, the samples exhibit variations in hand orientation. However, each user was still required to place the back of his or her hand on a fixed surface. After the preprocessing step, only $\approx 0.5\%$ of the samples were discarded. A total of 1937 ROIs were considered in our experiments.

4) Tongji Contactless Palmprint Dataset: The Tongji Contactless Palmprint Dataset (referred to as Tongji), collected by Tongji University, contains 6000 palmprint samples captured from 600 individuals with ages ranging from 20 to 50 years. The images were captured using the proprietary touchless acquisition device described in [45]. They are in 24-bit color and have dimensions of 800×600. Although the acquisition procedure required each user to place his or her hand inside an enclosure, the acquisition conditions were less constrained than those used to construct the CASIA and IITD databases since the hand was not touching any surface at the moment of acquisition. However, the illumination was controlled, and the position of the hand could vary only within a relatively small space. Consequently, all samples exhibit approximately the same hand orientation and similar illumination conditions. After the preprocessing step, $\approx 13\%$ of the samples were discarded. This is because the valleys between the fingers are not entirely visible in all images. A total of 5182 ROIs were considered in our experiments.

B. Evaluation Procedure and Error Metrics

To evaluate the accuracy of the proposed palmprint recognition method, we applied an n-fold cross-validation procedure, which is widely used for evaluating pattern recognition algorithms [74]. Specifically, we selected cross-validation with $n = 2$ and 5 repetitions [75], with one partition of the ROIs used for the training of the CNNs and one partition used for testing. The training and testing subsets each contained $\approx 50\%$ of the individuals in the database, selected randomly. The individuals in the training and testing subsets were disjoint. The feature extraction, classification, and matching steps were performed on the testing subset, and the results were averaged over the 5 iterations.

To comprehensively evaluate the accuracy of the proposed biometric system, we considered its performance in both the identification and verification modes. In the identification mode, the accuracy of a 1-NN classifier based on the Euclidean distance was evaluated using a leave-one-out procedure [74] on the feature vectors computed from the ROIs in the testing subset. This procedure enables the evaluation of how each sample compares against all remaining samples. As error metrics, we considered the classification accuracy, expressed as the percentage of correctly classified samples among the total number of samples, and the Cumulative Match Characteristic (CMC) curve. We chose these two error metrics because they are the most commonly used metrics for reporting the accuracy of a biometric system in the identification mode [1]. In the verification mode, we performed a technology evaluation [72] using a matching algorithm based on the Euclidean distance. For each individual, we considered 4 samples for enrollment and used the remaining samples for testing. Each round of matching was performed between a test sample and the 4 corresponding enrollment samples, and the minimum distance was taken as the final match score. This procedure is commonly applied for biometric acquisitions featuring significant intraclass variability (e.g., touchless and less-constrained acquisitions) since for each round of matching, it allows the most similar enrolled biometric sample to be selected [16]. As error metrics, we considered the equal error rate (EER) and the Receiver Operating Characteristic (ROC) curve [76] because they are the most commonly used metrics for reporting the accuracy of biometric systems in the verification mode [1].

A similar evaluation procedure was used for the methods in the literature that do not require a training phase. In these cases, we split the database using the same 2-fold cross-validation procedure, applied the method to the test subset, and evaluated the accuracy based on the resulting feature vectors.

C. Parameter Tuning and Sensitivity Analysis

We experimentally tuned the values of the parameter F, A', S, and V by varying them in the range $[5, 15]$, where the upper bound 15 was chosen to avoid memory demands exceeding the capabilities of the applied processing architecture, to select the parameter values resulting in the best classification accuracy. Specifically, we chose $F = 10$, $A' = 5$, $S = 10$, and $V = 15$. For PalmNet-Gabor, the chosen values of the parameters k_1 and k_2 were $k_1 = k_2 = F + A'$, and for PalmNet-GaborPCA, values of $k_1 = V = 15$ and $k_2 = F + A'$ were chosen. However, we believe that an experimental investigation with an optimized (e.g., C/CUDA-based) implementation of the approach could yield further insight.

We selected the values of the parameters u, v, μ, σ, a_0, r, and ψ by considering the optimal values found in the literature. Specifically, we chose $u = v = 128$ since this is a commonly used palmprint ROI size [27]; we selected $h_1 = h_2 = 35$, $\mu = 0.11$, and $\sigma = 5.6179$ because these represent the optimal values for a bank of fixed-scale Gabor filters [24]; and we considered $a_0 = 2$, $r = 1$, and $\psi = 2.4653$ based on the

optimal values for adaptive multiscale Gabor filters [25]. We experimentally tuned the values of b_1 and b_2 in the range $[1, u]$ and chose the values that resulted in the greatest recognition accuracy, namely, $b_1 = b_2 = 23$. Similarly, we tuned the values of m_1 and m_2 and chose the best values of $m_1 = m_2 = 15$.

The experimental procedure also included a sensitivity analysis of the parameters, which was performed by introducing variations of $\pm 20\%$ in the used values. In the worst case, we observed a decrease of $\approx 5\%$ in the recognition accuracy, demonstrating that the proposed approach can still be expected to outperform the other methods in the literature. We also tested variants of PalmNet-Gabor and PalmNet-GaborPCA in which only fixed-scale Gabor filters are considered in the Gabor-based filter tuning procedure, resulting in a decrease of at most $\approx 0.60\%$ in the recognition accuracy. Finally, we tested a variant of PalmNet-Gabor with 1 convolutional layer and 1 binarization layer, resulting in a decrease of at most $\approx 5\%$ in the recognition accuracy.

D. Filter Tuning

We visually examined the results of tuning the filters with the proposed method by training the proposed PalmNet on the considered databases. Fig. 6 shows the filters tuned using the Gabor-based tuning procedure described in Section III-B2 and the PCA-based tuning procedure described in Section III-B3. From this figure, it is evident that the proposed method tunes the filters differently for each database by adapting the scale and orientation of the filters to the characteristics of the training data.

E. Recognition Accuracy

We compared the recognition accuracies of the proposed PalmNet-Gabor and PalmNet-GaborPCA against those of the most recently reported methods in the literature. For the comparisons with local-texture-descriptor-based methods, we considered the CR-CompCode [6], LLDP [16], HOL [42], LDP [50], and LBP [40] methods. For the comparisons with DL-based methods, we considered PCANet [59] and the pretrained AlexNet, VGG-16, and VGG-19 CNNs [52]. We used the pretrained CNNs as feature extractors. We configured the methods using the parameters provided by their authors, when available. When both Gabor-based and MFRAT preprocessing were considered, we selected the Gabor-based version since it was the more accurate version in the vast majority of cases.

Table VI lists the recognition accuracies of the two CNNs designed based on the proposed method and those of the other considered methods in the literature for the identification mode, expressed in terms of the classification accuracy. As shown, the proposed CNNs PalmNet-Gabor and PalmNet-GaborPCA achieved the best accuracies on all considered touchless palmprint databases. In particular, PalmNet-GaborPCA achieved the highest classification accuracies among the considered methods.

Figure 7 shows the CMC curves, describing the identification rate as a function of rank, for all considered databases. The CMC curves confirm the superior accuracy of the proposed PalmNet-Gabor and PalmNet-GaborPCA compared to the methods in the literature.

TABLE VI
CLASSIFICATION ACCURACIES (%) OF THE PROPOSED CNNS COMPARED WITH THOSE OF OTHER METHODS IN THE LITERATURE

Ref.	Method	Type	Classification accuracy (%) CASIA	IITD	REST	Tongji
[40]	LBP	Text. descr.	99.02	92.81	76.56	99.71
[50]	LDP	Text. descr.	98.91	85.16	74.53	99.58
[42]	HOL	Text. descr.	99.18	95.90	78.54	99.64
[16]	$LLDP_1$	Text. descr.	99.08	96.87	79.06	99.73
	$LLDP_2$	Text. descr.	99.18	95.98	77.04	99.75
	$LLDP_3$	Text. descr.	98.91	96.72	77.22	99.76
[6]	CR-CompCode	Text. descr.	99.26	94.44	81.14	99.71
[59]	PCANet	DL (CNN)	99.76	98.35	92.94	99.78
	AlexNet	DL (CNN)	99.08	95.99	79.73	99.37
[52]	VGG-16	DL (CNN)	97.80	93.64	69.40	98.93
	VGG-19	DL (CNN)	97.57	94.45	68.43	98.46
-	**PalmNet-Gabor**	**DL (CNN)**	**99.77**	**99.06**	**96.59**	**99.80**
-	**PalmNet-GaborPCA**	**DL (CNN)**	**99.77**	**99.37**	**97.16**	**99.83**

Notes: Text. descr.: Local texture descriptor; DL: Deep learning; CNN: Convolutional neural network.

TABLE VII
EER VALUES (%) OF THE PROPOSED CNNS COMPARED WITH THOSE OF OTHER METHODS IN THE LITERATURE

Ref.	Method	Type	EER (%) CASIA	IITD	REST	Tongji
[40]	LBP	Text. descr.	4.37	10.79	19.64	1.70
[50]	LDP	Text. descr.	4.84	18.87	17.64	2.44
[42]	HOL	Text. descr.	4.62	6.70	13.79	0.41
[16]	$LLDP_1$	Text. descr.	3.54	3.76	11.61	0.36
	$LLDP_2$	Text. descr.	3.54	5.67	14.94	0.40
	$LLDP_3$	Text. descr.	4.38	5.18	13.40	0.54
[6]	CR-CompCode	Text. descr.	3.67	4.65	12.74	0.47
[59]	PCANet	DL (CNN)	1.63	1.37	8.91	0.20
	AlexNet	DL (CNN)	3.22	3.90	12.91	1.13
[52]	VGG-16	DL (CNN)	7.86	7.44	19.91	2.86
	VGG-19	DL (CNN)	7.84	7.75	20.46	3.96
-	**PalmNet-Gabor**	**DL (CNN)**	**0.71**	**0.71**	**3.59**	**0.19**
-	**PalmNet-GaborPCA**	**DL (CNN)**	**0.72**	**0.52**	**4.50**	**0.16**

Notes: Text. descr.: Local texture descriptor; DL: Deep learning; CNN: Convolutional neural network.

The proposed CNNs also exhibit uniform accuracy over all the considered databases, whereas traditional methods based on local texture descriptors show performance variations on different databases. For example, methods based on texture descriptors, while achieving high recognition accuracy on most databases, perform poorly on the REST database, which exhibits the greatest variations in hand position and orientation. By contrast, PalmNet-Gabor and PalmNet-GaborPCA are able to adapt to the specific characteristics of all databases, achieving a classification accuracy of $> 95\%$ in all cases.

Table VII lists the recognition accuracies of the proposed CNNs and those of the other methods in the literature for the verification mode, expressed in terms of the EER. As shown, the proposed PalmNet-Gabor and PalmNet-GaborPCA also achieved the best accuracies on the considered databases in this case.

Figure 8 shows the ROC curves for all considered databases. The curves illustrate the superior accuracies of the proposed PalmNet-Gabor and PalmNet-GaborPCA on all considered databases and for the majority of the false non-match rate (FNMR) and false match rate (FMR) values.

In all experiments, the proposed CNNs PalmNet-Gabor and PalmNet-GaborPCA achieved the best recognition accu-

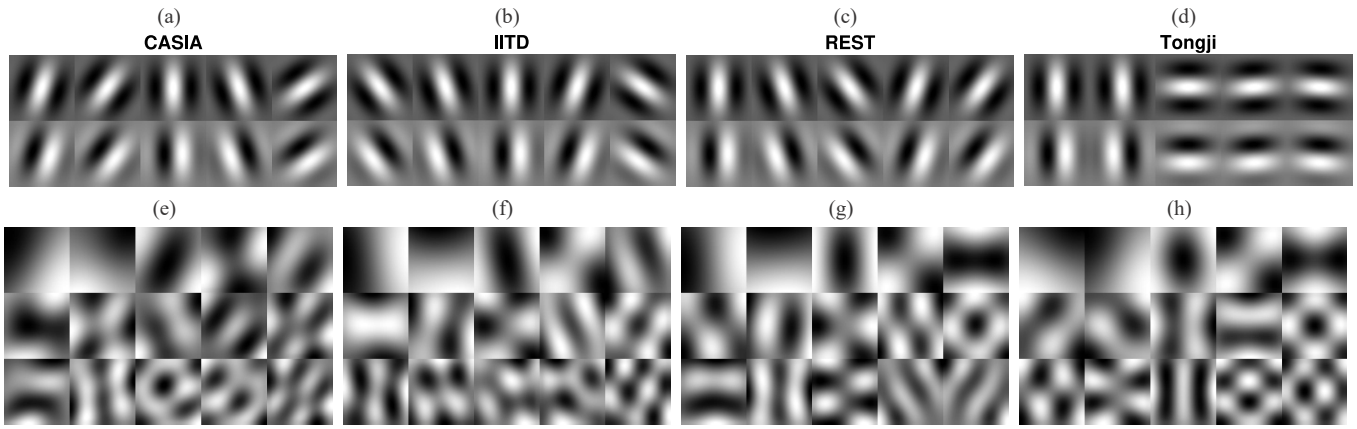

Fig. 6. Examples of filters tuned with the proposed PalmNet method. First row: results of the Gabor-based tuning procedure for the (a) CASIA, (b) IITD, (c) REST, and (d) Tongji databases (with both even- and odd-symmetric filters). Second row: results of the PCA-based tuning procedure for the (e) CASIA, (f) IITD, (g) REST, and (h) Tongji databases. It is evident that the proposed method tunes the filters differently for each database.

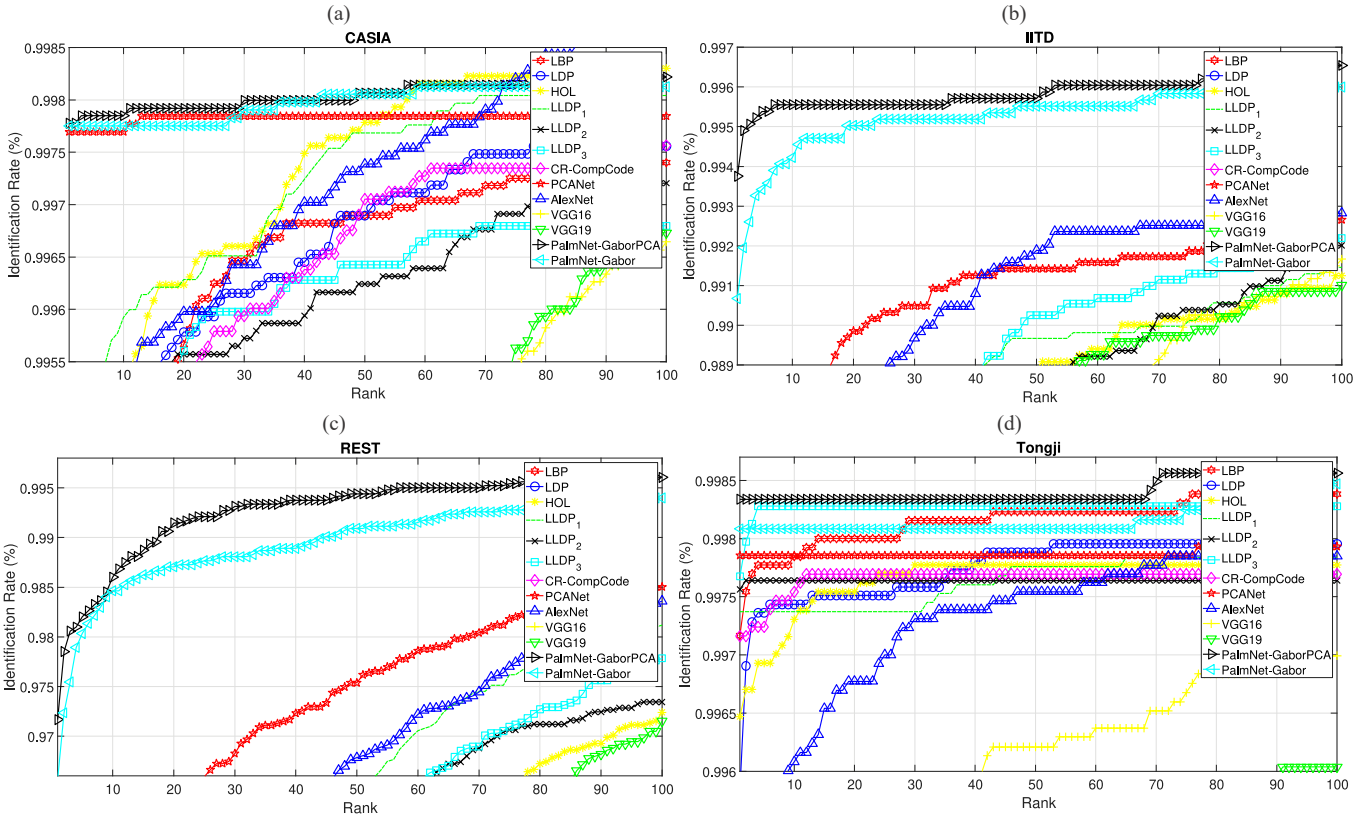

Fig. 7. CMC curves for the considered databases: (a) CASIA, (b) IITD, (c) REST, and (d) Tongji. It is evident that the proposed PalmNet-Gabor and PalmNet-GaborPCA outperform the other considered methods. In particular, PalmNet-Gabor and PalmNet-GaborPCA achieve the greatest performance improvements on databases captured with less-constrained acquisition procedures and exhibiting large variations in hand position (e.g., the REST database).

racies among the considered methods. In particular, PalmNet-GaborPCA demonstrated the best performance in the majority of cases. However, PalmNet-Gabor showed only slightly lower performance compared with PalmNet-GaborPCA, demonstrating the validity of the proposed Gabor-based filter tuning procedure.

Regarding the accuracy of the proposed PalmNet, it has been stated in the literature that high accuracy of a CNN often comes at the price of limited explainability [77]. However, in this work, we have attempted to propose a highly accurate yet simple CNN that is intrinsically interpretable. The proposed CNN has only two layers, it has no parameters learned through backpropagation or gradient descent, and it uses Gabor filters with a constrained shape. Its simplicity results in increased interpretability with respect to other CNNs in the literature. In fact, we believe that the higher accuracy of PalmNet can be attributed to two main factors: *i)* the integration of prior knowledge of the problem into the CNN and *ii)* the combination of the advantages of CNNs and local texture descriptors.

First, by integrating prior knowledge of the problem into the CNN, our method achieves a high recognition accuracy with a simple network with limited degrees of freedom, which can be trained with a limited quantity of data. Indeed, Gabor filters

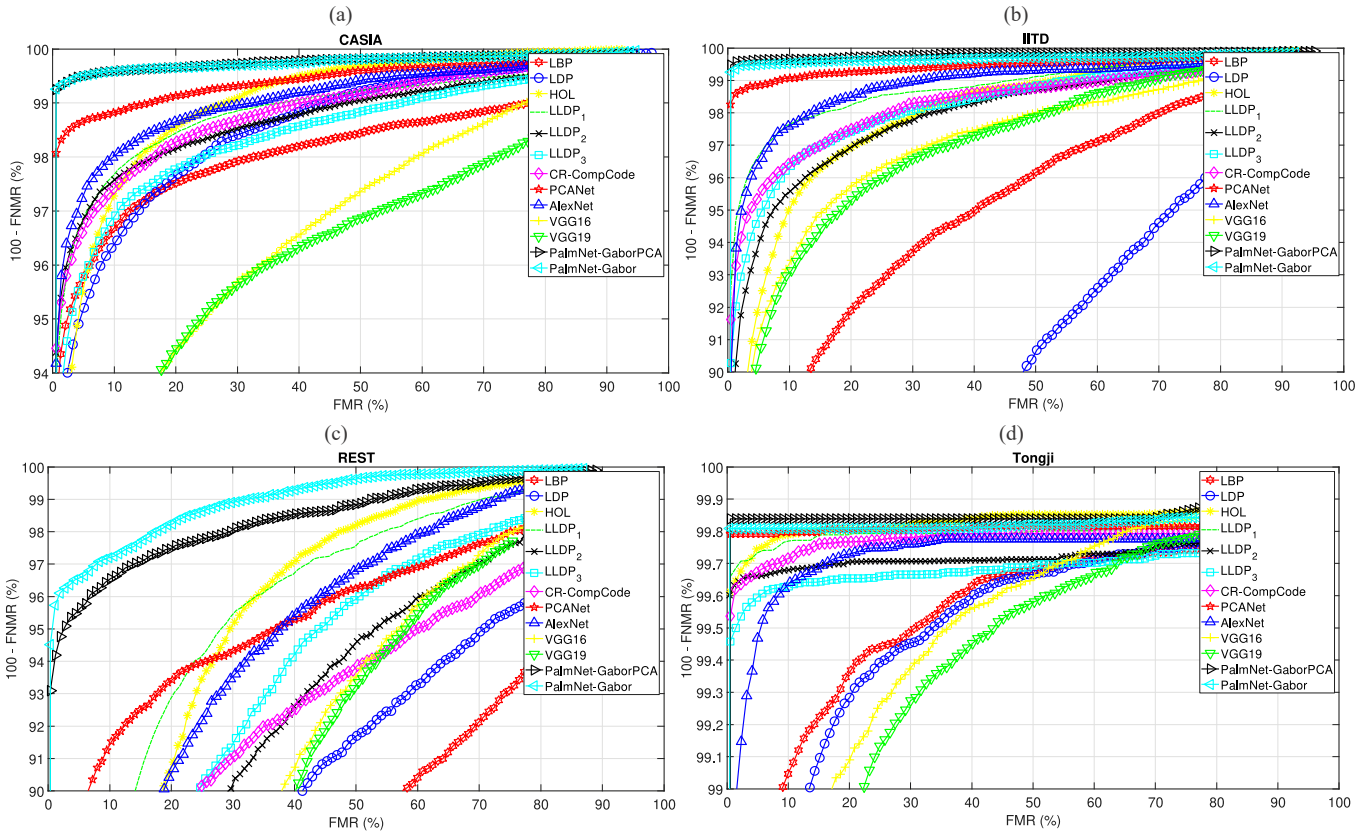

Fig. 8. ROC curves for the considered databases: (a) CASIA, (b) IITD, (c) REST, and (d) Tongji. It is evident that the proposed PalmNet-Gabor and PalmNet-GaborPCA outperform the other considered methods. In particular, PalmNet-Gabor and PalmNet-GaborPCA achieve the greatest performance improvements on databases captured with less-constrained acquisition procedures and exhibiting large variations in hand position (e.g., the REST database).

are currently used in state-of-the-art methods for palmprint recognition due to their ability to enhance the distinctive line patterns typical of palmprint samples. However, whereas the current methods in the literature consider only fixed-scale Gabor filters, whose parameters may not be optimal for each database, in our method, we extend the use of Gabor filters to consider the adaptively optimal set of multiscale filters that best enhances the features of each database. This optimal set is directly related to the orientation and thickness of the palmprint lines in the considered database.

Second, by combining the advantages of CNNs and local texture descriptors, the proposed method is endowed with adaptability and a multilayer structure, which are advantages typical of neural networks. In addition, the proposed method outputs a feature vector computed for each local region of an image, thus achieving robustness to local changes in illumination and scale, which is a typical advantage of methods based on local texture descriptors. The resulting feature vector represents the extent to which each image region contains palmprint lines with orientations and thicknesses matching the optimal set of Gabor filters tuned to a specific database.

F. Computation Time and Feature Size

We implemented all of the methods using the MATLAB R2018a prototyping environment and performed the tests on a personal computer with an Intel Core i7-7800X CPU @3.50 GHz, an NVIDIA Titan X Pascal GPU, 32 GB of RAM, and 64-bit Windows 10. The implementations were not optimized in terms of computational complexity. To evaluate the computation times, we did not use parallel computing strategies. To test the methods based on pretrained CNNs, we used the publicly available CUDA-based implementations for MATLAB.

TABLE VIII
AVERAGE COMPUTATION TIMES (IN SECONDS) FOR THE DIFFERENT STEPS OF THE PROPOSED PALMNET-GABORPCA

Step	Database			
	CASIA	IITD	REST	Tongji
CNN training	8813.61	4006.85	2921.96	8097.74
Feature extraction (all samples)	4665.63	1988.85	1523.67	4094.50
Classification and matching (all samples)	453.83	125.67	85.026	393.55
Feature extraction (1 sample)	1.60			
Matching (1 comparison)	0.01			

The feature vector size for PalmNet-Gabor and PalmNet-GaborPCA is computed as follows, similarly to other methods in the literature using PCA-based filters [22], [59]:

$$|H| = 2^{k_2} k_1 n_B = 2^{15} \cdot 15 \cdot 25 = 12\,288\,000 \ , \qquad (7)$$

where the value $n_B = 25$ is obtained as the number of nonoverlapping blocks with size $b_1 = b_2 = 23$ that fit in the input ROI image with size $u = v = 128$.

Table VIII shows the average computation times for the different steps of the proposed PalmNet-GaborPCA as well as the times needed to perform feature extraction for one

sample and the matching of two samples (1 comparison), averaged over all databases. From the table, it is evident that with the considered architecture, the feature extraction and matching steps for a single comparison require a total time of $(1.60) \times 2 + 0.01 = 3.21\ s$ for the proposed method. Thus, with high probability, it should be possible to use a trained PalmNet for the real-time recognition of individuals in a biometric system working in the verification mode, even when using a processing architecture with limited processing power.

Moreover, we believe that the use of optimized (e.g., C/CUDA-based) implementations could enable significant reductions in training time.

V. Conclusions

In this paper, we have proposed a novel method based on two newly developed CNNs for touchless palmprint recognition. The proposed method uses a novel approach for applying filters in a CNN based on Gabor responses and PCA and is trained using an innovative unsupervised procedure that does not require class labels, thus enabling the use of privacy-preserving palmprint images not associated with the identities of the corresponding individuals. The proposed CNNs are designed to extract highly discriminative features specific to palmprint samples and to adapt to databases captured using different devices.

In all cases, the application of the proposed CNNs on several touchless palmprint databases resulted in recognition accuracies higher than those achieved with other methods in the literature, demonstrating the validity of our approach for high-accuracy palmprint recognition. Moreover, the proposed CNNs exhibited more uniform accuracy results on heterogeneous databases compared with methods based on local texture descriptors, which may perform poorly on databases for which they were not designed. Specifically, we achieved a classification accuracy of $> 95\%$ on all considered databases, thus demonstrating the feasibility of also using the proposed method on future databases captured using different devices and acquisition procedures.

In this work, to demonstrate the validity of the proposed method for extracting high-accuracy features, we evaluated the accuracy achieved using simple classifiers and matching algorithms based on the Euclidean distance, which do not require training or have parameters to be tuned. However, future works should consider different classifiers and other distance measures.

References

[1] A. K. Jain, P. Flynn, and A. A. Ross, *Handbook of Biometrics*, 1st ed. Springer, 2010.

[2] L. Fei, G. Lu, W. Jia, S. Teng, and D. Zhang, "Feature extraction methods for palmprint recognition: A survey and evaluation," *IEEE Trans. Syst., Man, Cybern., Syst.*, pp. 1–18, 2018.

[3] L. Leng, M. Li, L. Leng, and A. B. J. Teoh, "Conjugate 2DPalmHash code for secure palm-print-vein verification," in *Proc. 2013 6th Int. Congress on Image and Signal Processing (CISP)*, December 2013, pp. 1705–1710.

[4] L. Leng, J. Zhang, M. K. Khan, X. Chen, and K. Alghathbar, "Dynamic weighted discrimination power analysis: a novel approach for face and palmprint recognition in DCT domain," *Int. Journal of Physical Sciences*, vol. 5, no. 17, pp. 2543–2554, 2010.

[5] Ö. Bingöl and M. Ekinci, "Stereo-based palmprint recognition in various 3D postures," *Expert Syst. Appl.*, vol. 78, pp. 74–88, 2017.

[6] L. Zhang, L. Li, A. Yang, Y. Shen, and M. Yang, "Towards contactless palmprint recognition: A novel device, a new benchmark, and a collaborative representation based identification approach," *Pattern Recognit.*, vol. 69, pp. 199–212, 2017.

[7] A. Genovese, V. Piuri, and F. Scotti, *Touchless Palmprint Recognition Systems*, ser. Advances in Information Security, S. Jajodia, Ed. Springer, September 2014, vol. 60.

[8] V. Kanhangad, A. Kumar, and D. Zhang, "A unified framework for contactless hand verification," *IEEE Trans. Inf. Forensic. Secur.*, vol. 6, no. 3, pp. 1014–1027, September 2011.

[9] L. Leng, M. Li, C. Kim, and X. Bi, "Dual-source discrimination power analysis for multi-instance contactless palmprint recognition," *Multimed. Tools Appl.*, vol. 76, no. 1, pp. 333–354, January 2017.

[10] G. K. O. Michael, T. Connie, and A. B. J. Teoh, "An innovative contactless palm print and knuckle print recognition system," *Pattern Recognit. Lett.*, vol. 31, no. 12, pp. 1708–1719, 2010.

[11] A. Kumar, "Toward more accurate matching of contactless palmprint images under less constrained environments," *IEEE Trans. Inf. Forensic. Secur.*, vol. 14, no. 1, pp. 34–47, January 2019.

[12] C. Zaghetto, M. Mendelson, A. Zaghetto, and F. d. B. Vidal, "Liveness detection on touchless fingerprint devices using texture descriptors and artificial neural networks," in *Proc. 2017 IEEE Int. Joint Conference on Biometrics (IJCB)*, October 2017, pp. 406–412.

[13] J. Y. Choi, Y. M. Ro, and K. N. Plataniotis, "Color local texture features for color face recognition," *IEEE Trans. Image Process.*, vol. 21, no. 3, pp. 1366–1380, March 2012.

[14] W. Jia, B. Zhang, J. Lu, Y. Zhu, Y. Zhao, W. Zuo, and H. Ling, "Palmprint recognition based on complete direction representation," *IEEE Trans. Image Process.*, vol. 26, no. 9, pp. 4483–4498, September 2017.

[15] G. Li and J. Kim, "Palmprint recognition with Local Micro-structure Tetra Pattern," *Pattern Recognit.*, vol. 61, pp. 29–46, 2017.

[16] Y.-T. Luo, L.-Y. Zhao, B. Zhang, W. Jia, F. Xue, J.-T. Lu, Y.-H. Zhu, and B.-Q. Xu, "Local line directional pattern for palmprint recognition," *Pattern Recognit.*, vol. 50, pp. 26–44, 2016.

[17] R. Das, E. Piciucco, E. Maiorana, and P. Campisi, "Convolutional neural network for finger-vein-based biometric identification," *IEEE Trans. Inf. Forensic. Secur.*, vol. 14, no. 2, pp. 360–373, February 2019.

[18] K. Sundararajan and D. L. Woodard, "Deep Learning for biometrics: A survey," *ACM Comput. Surv.*, vol. 51, no. 3, pp. 65:1–65:34, May 2018.

[19] R. Donida Labati, A. Genovese, E. Muñoz, V. Piuri, and F. Scotti, "A novel pore extraction method for heterogeneous fingerprint images using Convolutional Neural Networks," *Pattern Recognit. Lett.*, 2017.

[20] R. Donida Labati, A. Genovese, E. Muñoz, V. Piuri, F. Scotti, and G. Sforza, "Computational intelligence for biometric applications: a survey," *Int. Journal of Computing*, vol. 15, no. 1, pp. 40–49, 2016.

[21] R. Ramachandra, K. B. Raja, S. Venkatesh, S. Hegde, S. D. Dandappanavar, and C. Busch, "Verifying the newborns without infection risks using contactless palmprints," in *Proc. 2018 Int. Conf. on Biometrics (ICB)*, February 2018, pp. 209–216.

[22] A. Meraoumia, F. Kadri, H. Bendjenna, S. Chitroub, and A. Bouridane, "Improving biometric identification performance using PCANet deep learning and multispectral palmprint," in *Biometric Security and Privacy: Opportunities & Challenges in The Big Data Era*, R. Jiang, S. Almaadeed, A. Bouridane, D. Crookes, and A. Beghdadi, Eds. Cham: Springer, 2017, pp. 51–69.

[23] J. Svoboda, J. Masci, and M. M. Bronstein, "Palmprint recognition via discriminative index learning," in *Proc. 2016 23rd Int. Conf. on Pattern Recognition (ICPR)*, December 2016, pp. 4232–4237.

[24] W. K. Kong, D. Zhang, and W. Li, "Palmprint feature extraction using 2-D Gabor filters," *Pattern Recognit.*, vol. 36, no. 10, pp. 2339–2347, 2003.

[25] T. S. Lee, "Image representation using 2D Gabor wavelets," *IEEE Trans. Pattern Anal. Mach. Intell.*, vol. 18, no. 10, pp. 959–971, October 1996.

[26] S. Luan, C. Chen, B. Zhang, J. Han, and J. Liu, "Gabor Convolutional Networks," *IEEE Trans. Image Process.*, vol. 27, no. 9, pp. 4357–4366, September 2018.

[27] D. Zhang, W.-K. Kong, J. You, and M. Wong, "Online palmprint identification," *IEEE Trans. Pattern Anal. Mach. Intell.*, vol. 25, no. 9, pp. 1041–1050, September 2003.

[28] Hong Kong Polytechnic University, "Hong Kong Polytechnic University (PolyU) palmprint database," 2003. [Online]. Available: http://www4.comp.polyu.edu.hk/~biometrics/

[29] W. Jia, D.-S. Huang, and D. Zhang, "Palmprint verification based on robust line orientation code," *Pattern Recognit.*, vol. 41, no. 5, pp. 1504–1513, 2008.

[30] W. Zuo, Z. Lin, Z. Guo, and D. Zhang, "The multiscale competitive code via sparse representation for palmprint verification," in *Proc. 2010 IEEE Computer Society Conf. on Computer Vision and Pattern Recognition (CVPR)*, June 2010, pp. 2265–2272.

[31] Chinese Academy of Sciences, Institute of Automation, "CASIA Palmprint Image Database," 2009. [Online]. Available: http://english.ia.cas.cn/db/201611/t20161101_169936.html

[32] L. Fei, Y. Xu, W. Tang, and D. Zhang, "Double-orientation code and nonlinear matching scheme for palmprint recognition," *Pattern Recognit.*, vol. 49, pp. 89–101, 2016.

[33] Indian Institute of Technology Delhi, "IIT Delhi Touchless Palmprint Database (Version 1.0)," 2008. [Online]. Available: http://www4.comp.polyu.edu.hk/~csajaykr/IITD/Database_Palm.htm

[34] Z. Guo, D. Zhang, L. Zhang, and W. Zuo, "Palmprint verification using binary orientation co-occurrence vector," *Pattern Recognit. Lett.*, vol. 30, no. 13, pp. 1219–1227, 2009.

[35] L. Fei, B. Zhang, Y. Xu, and L. Yan, "Palmprint recognition using neighboring direction indicator," *IEEE Trans. Human-Mach. Syst.*, vol. 46, no. 6, pp. 787–798, December 2016.

[36] Y. Xu, L. Fei, J. Wen, and D. Zhang, "Discriminative and robust competitive code for palmprint recognition," *IEEE Trans. Syst., Man, Cybern., Syst.*, vol. 48, no. 2, pp. 232–241, February 2018.

[37] A. Ungureanu, S. Thavalengal, T. E. Cognard, C. Costache, and P. Corcoran, "Unconstrained palmprint as a smartphone biometric," *IEEE Trans. Consum. Electron.*, vol. 63, no. 3, pp. 334–342, August 2017.

[38] M. Aykut and M. Ekinci, "AAM-based palm segmentation in unrestricted backgrounds and various postures for palmprint recognition," *Pattern Recognit. Lett.*, vol. 34, no. 9, pp. 955–962, 2013.

[39] X. Wu, Q. Zhao, and W. Bu, "A SIFT-based contactless palmprint verification approach using iterative RANSAC and local palmprint descriptors," *Pattern Recognit.*, vol. 47, no. 10, pp. 3314–3326, 2014.

[40] X. Wang, H. Gong, H. Zhang, B. Li, and Z. Zhuang, "Palmprint identification using boosting Local Binary Pattern," in *Proc. 18th Int. Conf. on Pattern Recognition (ICPR)*, vol. 3, August 2006, pp. 503–506.

[41] A. Kumar, D. C. M. Wong, H. C. Shen, and A. K. Jain, "Personal verification using palmprint and hand geometry biometric," in *Audio- and Video-Based Biometric Person Authentication*, J. Kittler and M. S. Nixon, Eds. Springer, 2003, pp. 668–678.

[42] W. Jia, R. Hu, Y. Lei, Y. Zhao, and J. Gui, "Histogram of Oriented Lines for palmprint recognition," *IEEE Trans. Syst., Man, Cybern., Syst.*, vol. 44, no. 3, pp. 385–395, March 2014.

[43] L. Fei, J. Wen, Z. Zhang, K. Yan, and Z. Zhong, "Local Multiple Directional Pattern of palmprint image," in *Proc. 2016 23rd Int. Conf. on Pattern Recognition (ICPR)*, December 2016, pp. 3013–3018.

[44] University of Las Palmas de Gran Canaria, "Grupo de Procesado Digital de la Señal (GPDS) GPDS100Contactlesshands2Band database," 2011. [Online]. Available: http://www.gpds.ulpgc.es/

[45] Tongji University, "Tongji Contactless Palmprint Dataset," 2017. [Online]. Available: https://cslinzhang.github.io/ContactlessPalm/

[46] W. Jia, R.-X. Hu, J. Gui, Y. Zhao, and X.-M. Ren, "Palmprint recognition across different devices," *Sensors*, vol. 12, no. 6, pp. 7938–7964, 2012.

[47] S. Brahnam, L. C. Jain, L. Nanni, and A. Lumini, *Local Binary Patterns: New Variants and Applications*. Springer, 2013.

[48] L. Zhang, M. Yang, and X. Feng, "Sparse representation or collaborative representation: Which helps face recognition?" in *Proc. 2011 Int. Conf. on Computer Vision (ICCV)*, November 2011, pp. 471–478.

[49] N. Dalal and B. Triggs, "Histograms of Oriented Gradients for human detection," in *Proc. 2005 IEEE Conf. on Computer Vision and Pattern Recognition (CVPR)*, vol. 1, June 2005, pp. 886–893.

[50] T. Jabid, M. H. Kabir, and O. Chae, "Robust facial expression recognition based on Local Directional Pattern," *ETRI Journal*, vol. 32, no. 5, pp. 784–794, 2010.

[51] S. Murala, R. P. Maheshwari, and R. Balasubramanian, "Local Tetra Patterns: A new feature descriptor for content-based image retrieval," *IEEE Trans. Image Process.*, vol. 21, no. 5, pp. 2874–2886, May 2012.

[52] A. S. Tarawneh, D. Chetverikov, and A. B. Hassanat, "Pilot comparative study of different Deep features for palmprint identification in low-quality images," *CoRR*, vol. abs/1804.04602, 2018.

[53] A. Hassanat, M. Al-Awadi, E. Btoush, A. Al-Btoush, E. Alhasanat, and G. Altarawneh, "New mobile phone and webcam hand images databases for personal authentication and identification," *Procedia Manufacturing*, vol. 3, pp. 4060–4067, 2015.

[54] Autonomous Institute of Government of Maharashtra, "COEP palm print database," 2017. [Online]. Available: www.coep.org.in/resources/coeppalmprintdatabase

[55] Chinese Academy of Sciences, Institute of Automation, "CASIA multi-spectral palmprint database," 2007. [Online]. Available: http://www.cbsr.ia.ac.cn/english/MS_PalmprintDatabases.asp

[56] S. Minaee and Y. Wang, "Palmprint recognition using Deep Scattering Network," in *Proc. 2017 IEEE Int. Symp. on Circuits and Systems (ISCAS)*, May 2017, pp. 1–4.

[57] Hong Kong Polytechnic University, "Hong Kong Polytechnic University (PolyU) multispectral palmprint database," 2008. [Online]. Available: http://www4.comp.polyu.edu.hk/~biometrics/

[58] A. Krizhevsky, I. Sutskever, and G. E. Hinton, "ImageNet classification with Deep Convolutional Neural Networks," in *Proc. 25th Int. Conf. on Neural Information Processing Systems (NIPS)*, 2012, pp. 1097–1105.

[59] T. Chan, K. Jia, S. Gao, J. Lu, Z. Zeng, and Y. Ma, "PCANet: A simple Deep Learning baseline for image classification?" *IEEE Trans. Image Process.*, vol. 24, no. 12, pp. 5017–5032, December 2015.

[60] J. Bruna and S. Mallat, "Classification with scattering operators," in *Proc. IEEE Conf. on Computer Vision and Pattern Recognition (CVPR)*, June 2011, pp. 1561–1566.

[61] A. K. Jain, R. P. W. Duin, and J. Mao, "Statistical pattern recognition: a review," *IEEE Trans. Pattern Anal. Mach. Intell.*, vol. 22, no. 1, pp. 4–37, January 2000.

[62] R. A. Kirsch, "Computer determination of the constituent structure of biological images," *Computers and Biomedical Research*, vol. 4, no. 3, pp. 315–328, 1971.

[63] L. Leng, G. Liu, M. Li, M. K. Khan, and A. M. Al-Khouri, "Logical conjunction of triple-perpendicular-directional translation residual for contactless palmprint preprocessing," in *Proc. 2014 11th Int. Conf. on Information Technology: New Generations (ITNG)*, April 2014, pp. 523–528.

[64] G. K. O. Michael, T. Connie, and A. B. J. Teoh, "Touch-less palm print biometrics: Novel design and implementation," *Image Vis. Comput.*, vol. 26, no. 12, pp. 1551–1560, 2008.

[65] Y. Han, Z. Sun, F. Wang, and T. Tan, "Palmprint recognition under unconstrained scenes," in *Proc. 8th Asian Conf. on Computer Vision (AACV)*, 2007, pp. 1–11.

[66] L. Leng, F. Gao, Q. Chen, and C. Kim, "Palmprint recognition system on mobile devices with double-line-single-point assistance," *Personal Ubiquitous Comput.*, vol. 22, no. 1, pp. 93–104, February 2018.

[67] T. Chai, S. Wang, and D. Sun, "A palmprint ROI extraction method for mobile devices in complex environment," in *Proc. 2016 IEEE 13th Int. Conf. on Signal Processing (ICSP)*, November 2016, pp. 1342–1346.

[68] T. Connie, A. B. J. Teoh, M. G. K. Ong, and D. N. C. Ling, "An automated palmprint recognition system," *Image Vis Comput.*, vol. 23, no. 5, pp. 501–515, 2005.

[69] K. Ito, T. Sato, S. Aoyama, S. Sakai, S. Yusa, and T. Aoki, "Palm region extraction for contactless palmprint recognition," in *Proc. 2015 Int. Conf. on Biometrics (ICB)*, May 2015, pp. 334–340.

[70] C. Low, A. B. J. Teoh, and C. Ng, "Multi-fold Gabor, PCA, and ICA filter convolution descriptor for face recognition," *IEEE Trans. Circuits Syst. Video Technol.*, vol. 29, no. 1, pp. 115–129, January 2019.

[71] C. Low, A. B. J. Teoh, and K. Toh, "Stacking PCANet+: An overly simplified convnets baseline for face recognition," *IEEE Signal Process. Lett.*, vol. 24, no. 11, pp. 1581–1585, November 2017.

[72] J. Jang and H. Kim, "Performance measures," in *Encyclopedia of Biometrics*, S. Li and A. Jain, Eds. Springer, 2009, pp. 1062–1068.

[73] N. Charfi, H. Trichili, A. M. Alimi, and B. Solaiman, "Local invariant representation for multi-instance touchless palmprint identification," in *Proc. 2016 IEEE Int. Conf. on Systems, Man, and Cybernetics (SMC)*, October 2016, pp. 3522–3527.

[74] R. O. Duda, P. E. Hart, and D. G. Stork, *Pattern Classification (2Nd Edition)*. Wiley-Interscience, 2000.

[75] K. Nandakumar, Y. Chen, S. C. Dass, and A. Jain, "Likelihood ratio-based biometric score fusion," *IEEE Trans. Pattern Anal. Mach. Intell.*, vol. 30, no. 2, pp. 342–347, February 2008.

[76] A. Vedaldi and B. Fulkerson, "VLFeat: An open and portable library of computer vision algorithms," 2008. [Online]. Available: http://www.vlfeat.org/

[77] A. Adadi and M. Berrada, "Peeking inside the black-box: A survey on Explainable Artificial Intelligence (XAI)," *IEEE Access*, 2018.